Journal of Engineering for Gas Turbines and Power

Copy of e-mail Notification

Journal of Engineering for Gas Turbines and Power Published by ASME

Dear Author,

Congratulations on having your paper accepted for publication in the ASME Journal Program.

Your page proof is available in PDF format from the ASME Proof Download & Corrections site here:

http://115.111.50.156/jw/AuthorProofLogin.aspx?pwd=1855f583ae8d

Login: your e-mail address

Password: 1855f583ae8d

Please keep this email in case you need to refer back to it in the future.

You will need Adobe Acrobat Reader software to view the file. This is free software and a download link is provided when you log in to view your proofs.

Responsibility of detecting errors rests with the author. Please review the page proofs carefully and:

1. Answer any queries on the first page “Author Query Form”
2. Proofread any tables and equations carefully
3. Check to see that any special characters have translated correctly
4. Publication will not proceed until a response is received. If there are no corrections, a response is still required.

RETURNING CORRECTIONS:

Corrections must be returned using the ASME Proof Download & Corrections Submission Site (link above). You will be able to upload:

1. Annotated PDF
2. Text entry of corrections, with line numbers, in the text box provided
3. Additional files, if necessary.

SPECIAL NOTES:

Your Login and Password are valid for a limited time. Please reply within 48 hours.

Corrections not returned through the above website will be subject to publication delays. This e-proof is to be used only for the purpose of returning corrections to the publisher. If you have any questions, please contact: asme.cenveo@cenveo.com, and include your article no. (GTP-15-1315) in the subject line. This email should not be used to return corrections.

Approval of these proofs re-confirms the copyright agreement provision that all necessary rights from third parties for any copyrighted material (including without limitation any diagrams, photographs, figures or text) contained in the paper has been obtained in writing and that appropriate credit has been included.

Sincerely,

Mary O'Brien, Journal Production Manager

STATEMENT OF EDITORIAL POLICY AND PRACTICE

The Technical Committee on Publications and Communications (TCPC) of ASME aims to maintain a high degree of technical, literary, and typographical excellence in its publications. Primary consideration in conducting the publications is therefore given to the interests of the reader and to safeguarding the prestige of the Society.

To this end the TCPC confidently expects that sponsor groups will subject every paper recommended by them for publication to careful and critical review for the purpose of eliminating and correcting errors and suggesting ways in which the paper may be improved as to clarity and conciseness of expression, accuracy of statement, and omission of unnecessary and irrelevant material. The primary responsibility for the technical quality of the papers rests with the sponsor groups.

In approving a paper for publication, however, the TCPC reserves the right to submit it for further review to competent critics of its own choosing if it feels that this additional precaution is desirable. The TCPC also reserves the right to request revision or condensation of a paper by the author or by the staff for approval by the author. It reserves the right, and charges the editorial staff, to eliminate or modify statements in the paper that appear to be not in good taste and hence likely to offend readers (such as obvious advertising of commercial ventures and products, comments on the intentions, character, or acts of persons and organizations that may be construed as offensive or libelous), and to suggest to authors rephrasing of sentences where this will be in the interest of clarity. Such rephrasing is kept to a minimum.

Inasmuch as specific criteria for the judging of individual cases cannot, in the opinion of the TCPC, be set up in any but the most general rules, the TCPC relies upon the editorial staff to exercise its judgment in making changes in manuscripts, in rearranging and condensing papers, and in making suggestions to authors. The TCPC realizes that the opinions of author and editor may sometimes differ, and hence it is an invariable practice that no paper is published until it has been passed on by the author. For this purpose page proofs of the edited paper are sent to the author prior to publication in a journal. Changes in content and form made in the proofs by authors are followed by the editor except in cases in which the Society's standard spelling and abbreviation forms are affected.

If important differences of opinion arise between author and editor, the points at issue are discussed in correspondence or interview, and if a solution satisfactory to both author and editor is not reached, the matter is laid before the TCPC for adjustment.

Technical Committee on Publications and Communications (TCPC)
Reviewed: 05/2012

AUTHOR QUERY FORM

ASME SETTING THE STANDARD	**Journal: J. Eng. Gas Turbines Power** **Article Number: GTP-15-1315**	**Please provide your responses and any corrections by annotating this PDF and uploading it to ASME's eProof website as detailed in the Welcome email.**

Dear Author,

Below are the queries associated with your article; please answer all of these queries before sending the proof back to Cenveo. Production and publication of your paper will continue after you return corrections or respond that there are no additional corrections.

Location in article	Query / Remark: click on the Q link to navigate to the appropriate spot in the proof. There, insert your comments as a PDF annotation.
AQ1	Please provide postal code for all the affiliations.
AQ2	Please check the language edits made across the article.
AQ3	The figure parts (b), (c), (d), (e) have been changed to (a), (b), (c), (d) sequentially. So, please check and confirm.
AQ4	Kindly specify which section "in the previous sections" refers to here.
AQ5	Kindly specify which section "in the previous section" refers to here.
AQ6	Kindly specify which section "in previous sections" refers to here.
AQ7	Please provide page number in range for Ref. 4.
AQ8	Please provide city name for Ref. 5.
AQ9	Kindly provide DOI for Refs. 8, 10, 20.

Thank you for your assistance.

Alessio Suman[1]
Dipartimento di Ingegneria,
Università degli Studi di Ferrara,
Ferrara ■, Italy

AQ1

Mirko Morini
Dipartimento di Ingegneria Industriale,
Università degli Studi di Parma,
Parma ■, Italy

Rainer Kurz
Solar Turbines Incorporated,
San Diego, CA ■

Nicola Aldi
Dipartimento di Ingegneria,
Università degli Studi di Ferrara,
Ferrara ■, Italy

Klaus Brun
Southwest Research Institute,
San Antonio, TX ■

Michele Pinelli
Dipartimento di Ingegneria,
Università degli Studi di Ferrara,
Ferrara ■, Italy

AQ2

Pier Ruggero Spina
Dipartimento di Ingegneria,
Università degli Studi di Ferrara,
Ferrara ■, Italy

Estimation of the Particle Deposition on a Transonic Axial Compressor Blade

Solid particle ingestion is one of the principal degradation mechanisms in the compressor section of heavy-duty gas turbines. Usually, foulants in the ppm range, not captured by the air filtration system (0–2) μm cause deposits on blading and result in a severe performance drop of the compressor. It is of great interest to the industry to determine which areas of the compressor airfoils are interested by these contaminants as a function of the location of the power unit. The aim of this work is the estimation of the actual deposits on the blade surface in terms of location and quantity. The size of the particles, their concentrations, and the filtration efficiency are specified in order to perform a realistic quantitative analysis of the fouling phenomena in an axial compressor. This study combines, for the first time, the impact/adhesion characteristic of the particles obtained through a computational fluid dynamics (CFD) and the real size distribution of the contaminants in the air swallowed by the compressor. The blade zones affected by the deposits are clearly reported by using easy-to-use contaminant maps realized on the blade surface in terms of contaminant mass. The analysis showed that particular fluid-dynamic phenomena such as separation, shock waves, and tip leakage vortex strongly influence the pattern deposition. The combination of the smaller particles (0.15 μm) and the larger ones (1.50 μm) determines the highest amounts of deposits on the leading edge (LE) of the compressor airfoil. From these analyses, some guidelines for proper installation and management of the power plant (in terms of filtration systems and washing strategies) can be drawn.
[DOI: 10.1115/1.4031206]

Introduction

The quality and purity of the air entering the turbine is a significant factor in the performance and life of the gas turbine. The air is a continuous medium that contains and carries a large number of contaminants. The contaminants in the air are different in composition, size (pollen 50 μm, spores from 3 μm to 10 μm, and exhaust particle <0.1 μm), and quantity.

In order to minimize the performance loss of industrial gas turbines, an adequate filtration system that can limit the ingestion of contaminants by the power unit is required. Depending on the type of filtration system used, smaller particles (0–2) μm can enter the engine [1]. These smaller particles are too small to cause erosion issues but they are suitable for sticking to the blade surface and causing fouling.

Particle adhesion on the blade surface is a complex phenomenon that includes many aspects (materials, surface conditions, particle size, and impact dynamic). Particle sticking on the blade surfaces results in an increase of the thickness of the airfoil and the surface roughness. Both of these events change the flow-path inside the passage vanes. This leads to in particular: (i) an increment of boundary layer thickness, (ii) a decrement of the flow passage area, and (iii) modifications of 3D fluid-dynamic phenomena [2,3]. These phenomena result in a reduction of the compressor mass flow rate and consequently a reduction in the functioning of a turbine which results in a drop in overall gas turbine output of 5.5 MW in the case of a 40 MW class gas turbine [4].

After the particle deposition to the blade surface, the only method for recovering the performance of the compressor is washing operation [1]. Experimental results reported in Ref. [5] demonstrated that the process of washing was assumed to recover the output power up to 99.5%. Fouling can be removed by offline washing and slowed down by online washing. The decision to shut the engine down for offline washing is a balance between the lost production due to the lower power versus the lost production for shutting the engine down for a certain amount of time.

In this paper, an estimation of the deposits that afflict a blade surface is proposed. The quantitative analysis of the deposits on a blade surface is strongly related to realistic: (i) air contamination data, (ii) filtration efficiency, and (iii) particle adhesion. In particular, the paper is organized according to the following points:

— definition of the typical air contaminant concentration in the urban area as a function of (i) particle diameter and (ii) season;
— definition of the filtration efficiency as a function of (i) particle diameter and (ii) charge level of the electrostatic filter;
— definition of the particle adhesion to the blade surface as a function of (i) particle diameter and (ii) local position on the blade surface;
— calculation of the contaminant mass on the blade surface and quantitative analysis regarding the influence of external factors (such as season and filtration system) on a fouling rate.

Air Contaminant

The atmospheric aerosols are constituted by a suspension of solid (smoke, fumes, fly ash, dust, etc.) or liquid (mist, fog, etc.)

[1]Corresponding author.
Contributed by the Turbomachinery Committee of ASME for publication in the JOURNAL OF ENGINEERING FOR GAS TURBINES AND POWER. Manuscript received July 15, 2015; final manuscript received July 22, 2015; published online xx xx, xxxx. Editor: David Wisler.

in the atmosphere. The particle sizes can be categorized into seven classes:

- coarse solid (5–100) mm;
- granular solid (0.3–5) mm;
- coarse powder (100–300) μm;
- fine powder (10–100) μm;
- super fine powder (1–10) μm;
- ultrafine powder ∼1 μm; and
- nano particles ∼1 nm.

In general, fine particles refer mainly to a man-made action while the coarse particles refer mainly to a natural phenomenon. The aerosols assume a very wide range of concentrations (from 1 $\mu g/m^3$ to 100 $\mu g/m^3$) according to site location and time. In particular, the following relation summarizes the general rules [6]. Equation (1) reports the relation for the spatial ranges

$$\text{desert} > \text{urban area} > \text{ocean surface} > \text{pole} \quad (1)$$

Equation (2) reports the daily temporal ranges and Eq. (3) reports the weekly temporal ranges

$$\text{morning} > \text{evening} \quad (2)$$

$$\text{weekday} > \text{nonworking} \quad (3)$$

and finally, Eqs. (4) and (5) report the relation for the seasons

$$\text{winter} > \text{summer (caused heating system)} \quad (4)$$

$$\text{summer} > \text{winter (caused organic matter)} \quad (5)$$

The dispersed aerosols have different shapes as a function of their nature and source. In Ref. [7], there are detailed scanning electron microscope (SEM) pictures that report the shape of typical aerosols dispersed in the Shanghai urban summer atmosphere. Some SEM micrographs are reported in Fig. 1. The authors in Ref. [7] have reported a detailed chemical analysis related to the air contaminant, and have emphasized the characterization of the *ultrafine* particles. The results demonstrated that the Shanghai urban area is dominated by a *fine* particle (0.1–2.5) μm constituted by soot aggregates and fly ashes.

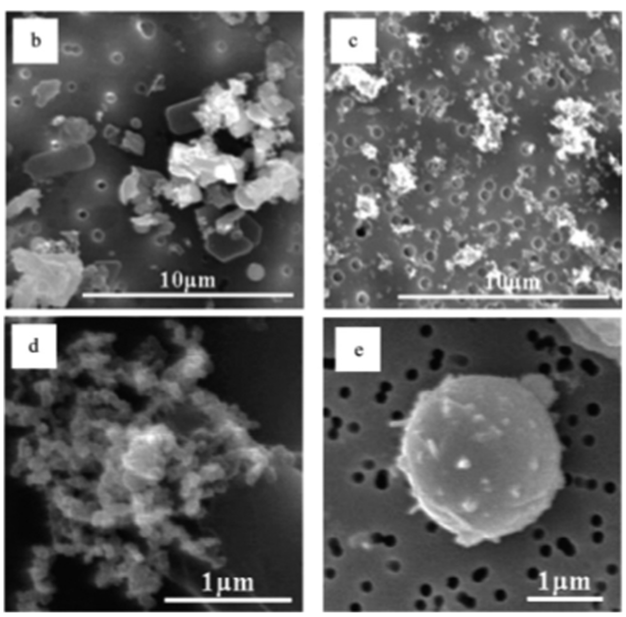

AQ3

Fig. 1 SEM micrographs of size-segregated particles: (*a*) fine particles, (*b*) ultrafine particles, (*c*) soot aggregates, and (*d*) fly ash [7]

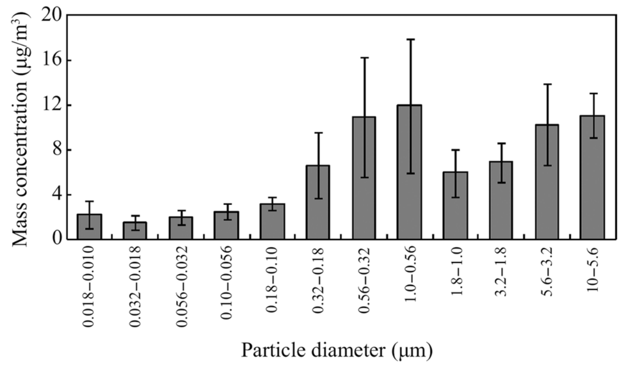

Fig. 2 Mass concentrations of size-segregated particles collected in the Shanghai atmosphere [7]

In Ref. [7], there is also a mass characterization of the different size airborne particles. The mass level characterization is reported in Fig. 2. This characterization will be used in this work to analyze the mass deposits on a compressor blade surface in a configuration named Urban (U).

In order to realize as wide a fouling sensitivity analysis as possible, not only the mass level characterizations reported in Fig. 2 are considered in this work. In some cases, the power units work in highly contaminated areas, due to local chimney, plumes and/or soils. For these reasons, the mass level characterization reported in Ref. [8] is also taken into account. The authors in Ref. [8] reported air contaminant characterization of the Xuanwei, Yunnan province (China) divided into two periods: spring season and winter season. This area is characterized by pollutants emitted by local coal combustion. The mass level characterization, as a function of the season, is reported in Fig. 3. The authors in Ref. [8] have found that the total mass concentrations of the size-resolved particles collected in spring were higher than those in early winter. The high concentration found in the spring time is not affected by the spore because the spore diameter is equal to 50 μm, and therefore, out of the sampled range. These characterizations will be used in this work to analyze the mass deposits on a compressor blade surface in a configuration named industrial spring (IS) and industrial winter (IW).

Filtration Systems

The inlet filtration system cleans the air entering the gas turbine. Poor quality inlet air can significantly impact the operation, performance, and life of the gas turbine. The gas turbine is affected by various substances in the inlet air depending on their composition and their particle size. As reported in Ref. [9], there are six common consequences of poor inlet air filtration: foreign

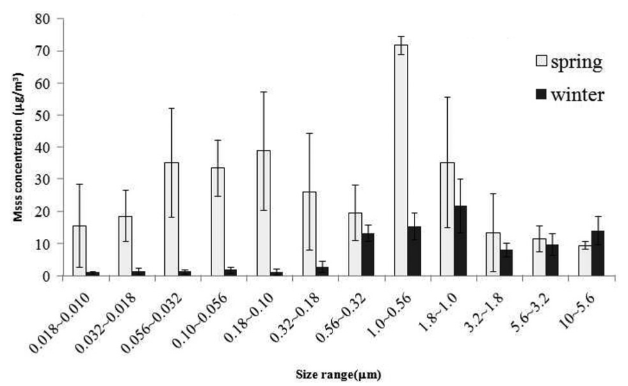

Fig. 3 Mass concentrations of size-segregated particles collected in the Xuanwei atmosphere [8]

object damage, erosion, fouling, turbine blade cooling passage plugging, particle fusion and corrosion (hot and cold). In contrast, the negative side of filtration is that whatever is placed in the path of air coming into the gas turbine causes a pressure loss, resulting in reduced performance or efficiency of the machine.

The filtration system should be selected based on the operational philosophy and goals for the turbine, the contaminants present in the ambient air, and expected changes in the contaminants in the future due to temporary emission sources or seasonal changes.

In order to capture different types of particles, filtration systems use many different mechanisms. Each filter in fact has various different mechanisms working together to remove the particles. The filter media, fiber size, packing density of the media, particle size, and electrostatic charge influence how the filter removes particles. The consolidated mechanism used in the air filtration systems are: (i) inertial impaction, (ii) diffusion, (iii) interception, (iv) sieving, and (v) electrostatic charge. The inertial impaction is applicable to particles larger than 1 μm in diameter. The inertia of the large heavy particles in the flow stream causes the particles to continue on a straight path as the flow stream moves around a filter fiber. The diffusion mechanism is effective for very small particles typically less than 0.5 μm in size. Particularly in turbulent flow, the path of small particles fluctuates randomly about the main stream flow. As these particles diffuse in the flow stream, they collide with the fiber and are captured. Interception occurs with medium sized particles that are not large enough to leave the flow path due to inertia or not small enough to diffuse. The particles will follow the flow stream where they will touch a fiber in the filter media and be trapped and held. Sieving is the situation where the space between the filter fibers is smaller than the particle itself, which causes the particle to be captured and contained. The last mechanism is related to the electrostatic charge. The filter works through the attraction of particles to a charged filter. Filters always lose their electrostatic charge over time because the particles captured on their surface occupy charged sites, therefore neutralizing their electrostatic charge. When the filter is loaded filtration efficiency increases while when the charge diminishes, filtration efficiency drops, especially for small particles.

An extensive report on filtration efficiency can be found in Ref. [9] where it can be seen that for the particles with dimensions less than $\approx 2\,\mu$m, and in more detail, with diameters in the range of (0.1–1.0) μm, conventional filtration systems will not entirely prevent these small particles from entering the gas turbine, and therefore, may cause fouling [1].

Figure 4 shows a comparison of a filter's total efficiency based on the various filtration mechanisms that are applied as a function of the particle diameter. The figure shows the difference between

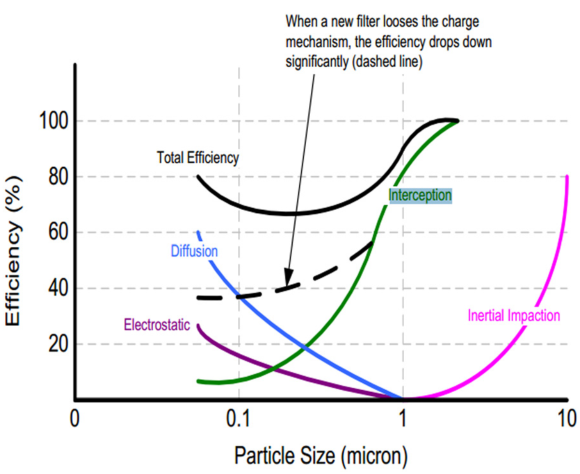

Fig. 4 Combination of filtration mechanisms to obtain filter efficiency at various particle sizes [9]

the filter's efficiency curves as a function of the electrostatic charge.

The trends reported in Fig. 4 will be used in this work to calculate the air contaminant concentration at the inlet section of the compressor. Starting with the data mentioned in the previous paragraph related to contaminant concentration in the air, by using the filtration efficiency reported in Fig. 4, it is possible to put into effect the air filtration systems for the analysis of the mass deposits on the blade surface.

Particle Adhesion

The details on how small particles entering the gas turbine reach the blade surface and stick are not fully and quantitatively understood. Evaluation of fouled compressors has revealed contamination both on the suction side (SS) and the pressure side (PS) of the compressor blades. The fouling effects on compressor performance are different as a function of the blade side [1].

The authors in Ref. [10] reported an investigation of compressor blade contamination for a Nuovo Pignone MS5322 R(B) gas turbine engine. This power unit operated for a long time without blade washing but only the first five to six stages of 16 are subjected to blade fouling due to deposits. The inlet guide vane blades, as well as the rotor and stator blades of the first stage, have more deposits on the blade convex side. The deposits masses on blades of the other stage are approximately equal for the convex and concave sides. The deposits masses decrease from the first to the sixth stage. From the seventh stage, the amount of deposits on blades is insignificant. The authors highlighted that the deposits amount is greater on the stator blades than on the rotor blades, due to the cleaning effects provided by the centrifugal forces on the dirt particles. Centrifugal forces have also characterized the results reported in Ref. [11]. The authors reported the location of salt deposits in General Electric J85-13 axial compressor. The experimental tests have shown that the salt deposits were mainly found along the LE of the first four stages and on the PS of the stator vanes along the hub. The salt deposits were generated by the salt carried by the water droplets and, for this reason, significantly less deposits were observed on the rotor blades compared to the stator vanes.

In literature, regarding the fouling application and the ultrafine powder in axial compressors, there are some experimental results. The authors in Refs. [5], [12], and [13] have reported some experimental measurements with regard to the deposition on the axial compressor blade surface. All of the experimental applications related to the fouling phenomenon are affected by numerous problems summarized as follows: (i) actual conditions of the contaminants and the work environment of the compressor, (ii) size of the experimental test bench, in particular even if the cascade and velocities are scalable, the particle dimension is not scalable and its ratio with respect to the cascade and velocities must be respected and, as reported by Ref. [14], on the condition of keeping the aerodynamic and geometrical similarity, the compressor of a smaller size (a model) is more sensitive to fouling than a full-scale one, (iii) rotational velocity of the cascade (neglected in nearly all experimental apparatus) influences the dynamic and the kinematic characteristics of the particle impact, (iv) the modification of the interface between the particle and the blade in order to accelerate the fouling process limiting the validity of the results, and finally (v) the lack of particle count, in particular the lack of the ratio between the injected particles and the stuck particles. For these reasons, the fouling phenomenon is not fully understood.

An alternative solution can be found by using results obtained in different research fields. Interdisciplinary research can represent a new frontier for a considerable up-grade in the fouling investigation. In fact, some very interesting results and analysis of microparticle adhesion can be found in astrophysics research (preplanetary dust). The uniqueness and usefulness of these studies is that the particle velocities, materials, and dimensions are in the same range as those responsible for the fouling phenomenon.

In this paper, the numerical results reported in Ref. [15] will be used to estimate the mass deposition on a compressor blade. In Ref. [15], the authors have reported (i) an extensive analysis of the kinematic behavior of particles responsible for the fouling phenomenon and (ii) a quantitative analysis of particle adhesion. The analysis is directly related to the particles which have a diameter in the range of (0.15–2.00) μm and provide the deposits mass flow rate that affects the blade surface. In order to extend the results reported in Ref. [15] (which refer to the instantaneous impact) to a realistic condition (which refer to the impact during the compressor operation), a new index is introduced.

The results reported in Ref. [15] are related to the numerical results reported in Ref. [16] and to the experimental results reported in Ref. [17]. In particular, the results reported in Ref. [17] have particle velocity, size, and materials similar to those causing fouling phenomena. The particle adhesion is established by using the sticking probability (SP) magnitude defined as a function of the normal particle impact velocity. With this approach, the authors wish to emphasize that the particle impacts are different from each other and, in order to provide a macroscopic evaluation of the results, a statistic/probabilistic approach is the best way. This procedure allows the identification of the dangerous particles (that will be able to stick) with respect to fouling phenomenon. In general, smaller particles have a wider range of normal impact velocity for which, there is a high probability that particle impact becomes a permanent adhesion. More details can be found in Refs. [15] and [17].

Fouling Analysis

In this section, the authors will report the data used for the estimation of the mass deposits on a blade surface. The data are directly related to the information and sources reported in the previous sections.

AQ4

Air Contaminant. By using the literature data reported above [7,8], it is possible to define the air contaminant concentration at the inlet section of the air filtration system. Table 1 summarizes the literature data, in particular the table reports the mass concentration as a function of the particle diameter range and its average.

Filtration Systems. By using the literature data reported above [1,9], it is possible to define the filtration efficiency as a function of the particle diameter. In this paper, two conditions are taken into account: (i) optimal charge (OC) condition (high efficiency) and (ii) poor charge (PC) condition (low efficiency) of the electrostatic filters.

As mentioned above, the particle adhesion data refers to the results reported in Ref. [15], and for this reason, the filtration efficiency is defined for the analyzed particle diameter. The filtration efficiency values as a function of the particle diameter are reported in each table.

Table 1 Mass concentration as a function of the particle diameter for U, IS, and IW environment

d_{min} (μm)	d_{max} (μm)	d_{ave} (μm)	χ_U (μg/m^3)	χ_{IS} (μg/m^3)	χ_{IW} (μg/m^3)
0.010	0.018	0.014	2.50	16.50	2.00
0.018	0.032	0.025	1.50	18.50	2.00
0.032	0.056	0.044	2.00	35.00	2.00
0.056	0.100	0.078	2.50	33.00	2.50
0.100	0.180	0.140	3.25	39.00	2.00
0.180	0.320	0.250	6.75	26.00	3.00
0.320	0.560	0.440	11.00	19.50	13.00
0.560	1.000	0.780	12.00	72.00	15.25
1.000	1.800	1.400	6.00	35.00	21.50
1.800	3.200	2.500	7.00	13.50	8.00
3.200	5.600	4.400	10.25	11.50	10.00
5.600	10.000	7.800	11.00	9.50	14.00

Table 2 Urban, OC

d_p (μm)	χ_p at air (#/m^3)	η_f (%)	χ_p at inlet (#/m^3)	P (#/s)
0.15	7.2×10^8	68	2.3×10^8	4.3×10^9
0.25	3.2×10^8	67	1.1×10^8	2.0×10^9
0.50	6.6×10^7	72	1.8×10^7	3.4×10^8
1.00	9.0×10^6	91	8.2×10^5	1.5×10^7
1.50	1.3×10^6	98	2.7×10^4	5.0×10^5

Table 3 IS, OC

d_p (μm)	χ_p at air (#/m^3)	η_f (%)	χ_p at inlet (#/m^3)	P (#/s)
0.15	8.6×10^9	68	2.7×10^9	5.2×10^{10}
0.25	1.2×10^9	67	4.1×10^8	7.7×10^9
0.50	1.2×10^8	72	3.2×10^7	6.1×10^8
1.00	5.4×10^7	91	4.9×10^6	9.2×10^7
1.50	7.7×10^6	98	1.5×10^5	2.9×10^6

Table 4 IW, OC

d_p (μm)	χ_p at air (#/m^3)	η_f (%)	χ_p at inlet (#/m^3)	P (#/s)
0.15	4.4×10^8	68	1.4×10^8	2.6×10^9
0.25	1.4×10^8	67	4.7×10^7	8.9×10^8
0.50	7.8×10^7	72	2.2×10^7	4.1×10^8
1.00	1.1×10^7	91	1.0×10^6	2.0×10^7
1.50	4.8×10^6	98	9.5×10^4	1.8×10^6

Table 5 Urban, PC

d_p (μm)	χ_p at air (#/m^3)	η_f (%)	χ_p at inlet (#/m^3)	P (#/s)
0.15	7.2×10^8	49	3.7×10^8	6.9×10^9
0.25	3.2×10^8	47	1.7×10^8	3.2×10^9
0.50	6.6×10^7	54	3.0×10^7	5.7×10^8
1.00	9.0×10^6	82	1.6×10^6	3.0×10^7
1.50	1.3×10^6	93	9.5×10^4	1.8×10^6

Thanks to the sampled ranges reported in Refs. [7] and [8], it is possible to link the analyzed particle diameters reported in Ref. [12]. Then, combining the mass concentration values (U, IS, and IW) and the filtration efficiency (OC and PC), the contaminant concentration at the inlet section of the compressor can be calculated for the six considered cases (Tables 2–7).

In order to realize a comparative analysis, some hypotheses must be defined:

— The density of the contaminant is imposed equal to 3000 kg/m^3. This value is obtained by a mass-weighted average of the air contaminant proposed in Refs. [7] and [8].

— The filtration efficiency for the particles with $d_p < 0.15\,\mu$m and $d_p > 1.50\,\mu$m is imposed equal to 100% (in agreement with [1,9]).

— In order to calculate the number of particles swallowed by the compressor, the volume flow rate at the best efficiency point equal to 18.88 m^3/s is imposed.

Table 6 IS, PC

d_p (μm)	χ_p at air (#/m^3)	η_f (%)	χ_p at inlet (#/m^3)	P (#/s)
0.15	8.6×10^9	49	4.4×10^9	8.3×10^{10}
0.25	1.2×10^9	47	6.6×10^8	1.2×10^{10}
0.50	1.2×10^8	54	5.3×10^7	1.0×10^9
1.00	5.4×10^7	82	9.6×10^6	1.8×10^8
1.50	7.7×10^6	93	5.5×10^5	1.0×10^7

Table 7 IW, PC

d_p (μm)	χ_p at air (#/m^3)	η_f (%)	χ_p at inlet (#/m^3)	P (#/s)
0.15	4.4×10^8	49	2.3×10^8	4.3×10^9
0.25	1.4×10^8	47	7.6×10^7	1.4×10^9
0.50	7.8×10^7	54	3.5×10^7	6.7×10^8
1.00	1.1×10^7	82	2.0×10^6	3.8×10^7
1.50	4.8×10^6	93	3.4×10^5	6.4×10^6

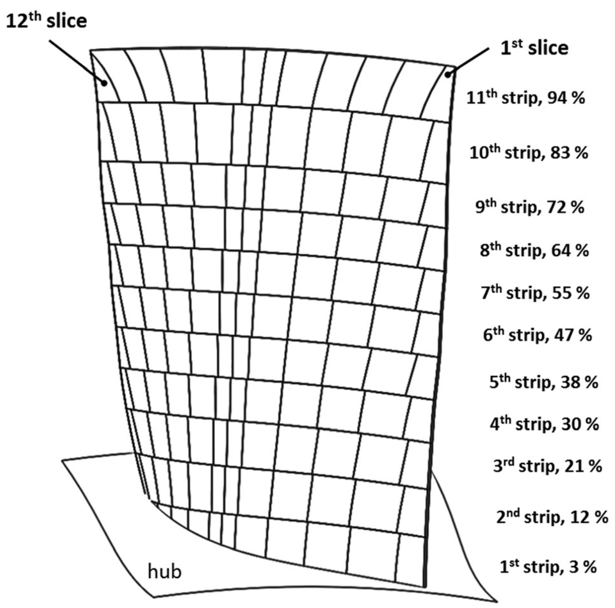

Fig. 5 Subdivision of the blade surface: eleven strips with its correspondent percentage of the blade span and twelve slices

Particle Adhesion. As mentioned above, this paper provides an estimation of the mass flow rate deposits (timewise scenario) and for this reason, the results reported in Ref. [15] must be processed in a different way. In Ref. [15] in fact, the results refer to the particle impact (instantaneous scenario), and the SP threshold limit imposed equal to 0.5 represents a useful discerning value to establish which particles stick or bounce.

In order to attribute the instantaneous scenario to the timewise scenario, the dangerous index (DI) is proposed. This new index refers to a specific amount of particles (that have a nonzero value of SP) that impact on a specific blade area. The DI is defined as the product between the ratio n and the average value of the

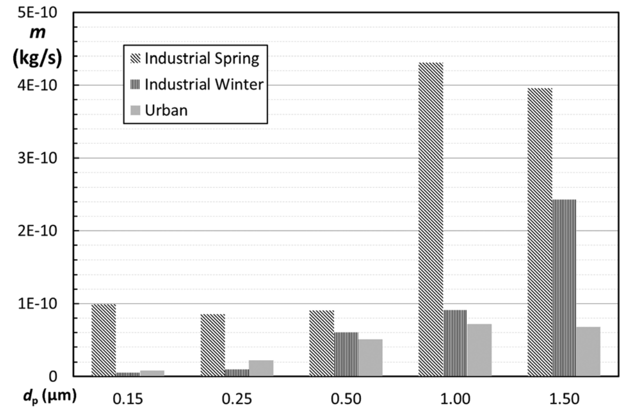

Fig. 7 Contaminant mass on the PS without filtration system

particle sticking probability SP_{ave}. The ratio n is defined as the ratio between the amount of particles that hit the blade area with a $SP > 0$ and the amount of particles that enter the compressor. This definition is in agreement with the sticking coefficient reported in Ref. [18] that represents the mass fraction of incident particles to a surface that are retained on that surface.

SP used in this analysis does not consider the influence of the relative humidity and in particular the influence of the wetness in the passage vanes. In general, particles that impact on wet surface have more chance to stick there [1] but, at the same time, the droplets that result on the blade surface (due to the humidity and/or to the inlet depression for the early stages) could drag the airborne contaminants from the rotor to the stator surfaces. The influence of the centrifugal forces is well described in Ref. [10] and its greatest "cleaning" effect is well reported in Ref. [11]. In the latter analysis, the salt deposits, generated by the salt carried by the water droplets, are localized in greater quantity on the stator surfaces instead of the rotor surfaces.

In order to cover the entire particle diameter range from 0.15 μm to 1.50 μm, the results reported in Ref. [15] must be completed by the data related to the SP for $d_p = 0.15\,\mu$m and $d_p = 1.50\,\mu$m.

The authors highlight that the particle characteristics used in Ref. [17] are quite different compared to the classic particle characteristics involved in the fouling phenomena. In particular, the silicon carbide particles [17] have a very high level of hardness and this implies that the rebound properties could be different from those found in the real fouling applications.

The CFD numerical simulations performed by Suman et al. [15,16] refer to a particle density equal to 2560 kg/m^3 instead of a density equal to 3000 kg/m^3 assumed in this analysis. The different density allows the evaluation of the actual contaminant mass

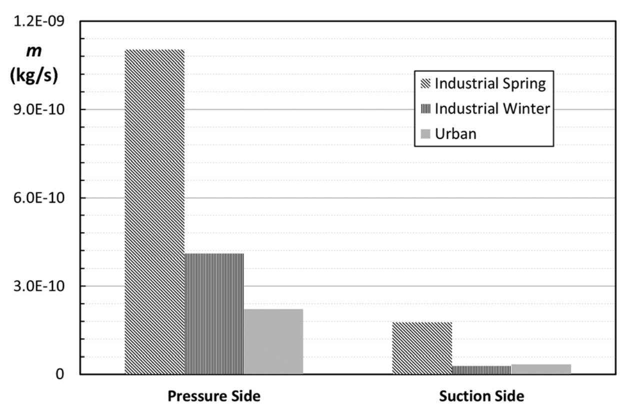

Fig. 6 Contaminant mass on the blade surface without filtration system

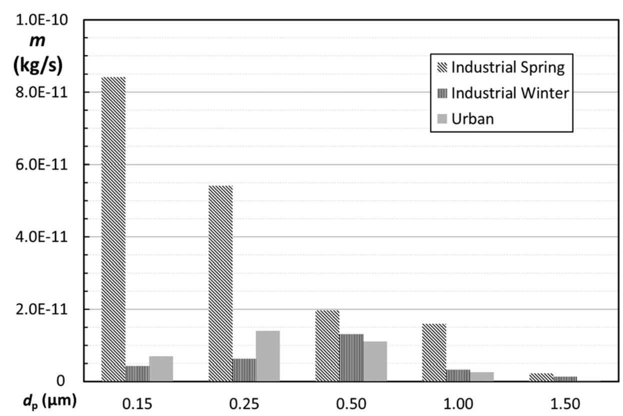

Fig. 8 Contaminant mass on the SS without filtration system

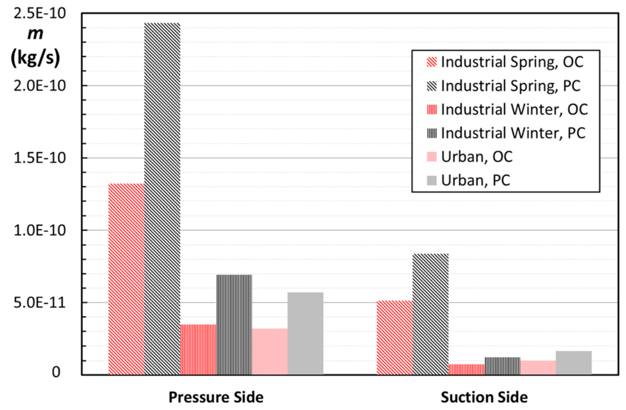

Fig. 9 Contaminant mass on the blade surface with filtration system

that afflicts the blade surface and at the same time does not diminish the validity of the numerical results.

In the following paragraphs the deposits on the blade surface are analyzed in two different manners: (i) deposits divided by the blade side (pressure or suction) and (ii) deposits divided by a very fine discretization of the blade surface (mesh).

In Fig. 5, the mesh realized on the blade surface is reported. From Fig. 5, the subdivision of the blade surface is clearly seen as: from hub to shroud with 11 strips while from LE to trailing edge with 12 slices.

Results

The results refer to two analyses. The first one is the blade contamination analysis in which the sensitivity analyses as a function of the blade side (pressure or suction) are reported. The second one is the calculation and representation of the overall deposits on the blade surface.

Blade Contamination. In this section, the authors have reported the analysis related to the deposits on the pressure and SS, as a function of the conditions mentioned above. The analysis refers to the quantification of the deposits on the blade surfaces in order to highlight the conditions that are more dangerous for the compressor. As reported by Morini et al. [19], the same deposits generate different performance drops as a function of the blade side. The deposits on the SS are more dangerous than the deposits on the PS.

The first analysis is carried out in order to set the reference. In fact, the results reported in Figs. 6–8 show the blade contamination in the absence of the filtration systems.

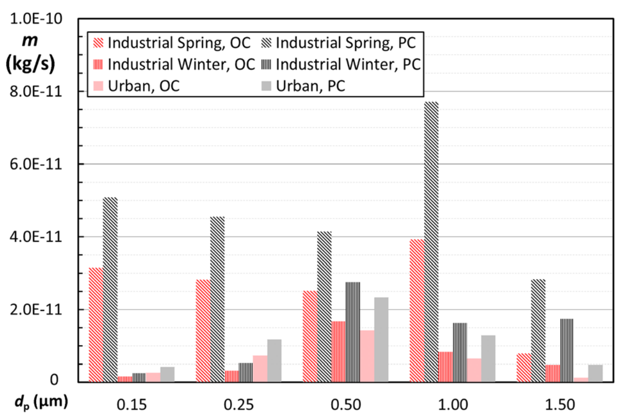

Fig. 10 Contaminant mass on the PS with filtration system

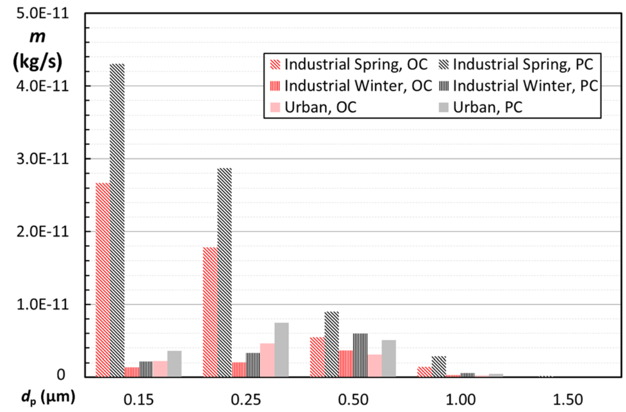

Fig. 11 Contaminant mass on the SS with filtration system

The values in Figs. 6–8 are the results of the combination between the contaminant concentration in the air (Table 1) and the DI values. The values refer to mass per second that sticks to the blade surface. The considered particle diameters are those that have a filtration efficiency of less than 100%.

From Fig. 6, it is clearly visible that the PS is more contaminated than the SS, in all conditions. In the PS, the deposits generated by the IW condition are higher than those generated by the Urban condition. In contrast, in the sides, the Urban condition is more dangerous than the IW condition. The higher deposition on the SS corresponds to the IS condition as well as on the PS.

In Figs. 6 and 7, the differences in terms of particle diameter are reported for the PS and the SS, respectively. The PS is more contaminated by particles with a diameter equal to 1.00 μm in the IS condition as well as the SS in which the most dangerous particles have a diameter equal to 0.15 μm. In this case, it is clearly visible how the combination of the contaminant concentration and the SP values (represented by the DI) determines different results as a function of the blade side. In the PS the bigger particles are responsible for higher blade side contamination. These particles ($d_p = 1.00\ \mu$m and $d_p = 1.50\ \mu$m) hit the PS with an SP_{ave} which is lower than the SP_{ave} of the smaller particles but the higher number of impacts determine a very dangerous condition for this blade side. The impact results are reported by Suman et al. [15]. In the sides, the particle contributions are more similar and, fixing the condition, the dangerous diameter changes. In fact, the diameter of the dangerous particles for the IS condition is 0.15 μm, but for the IW condition it is 0.50 μm and finally, for the Urban condition it is 0.25 μm.

These results confirm the requirement of (i) different filtration systems, in order to prevent the deposits in both of the blade sides at the same time and (ii) proper filtration system as a function of the location of the power unit, as reported in Ref. [9].

Figure 9 reports the results related to the blade contamination with filtration systems. Two conditions are reported: OC and PC of the filtration system. The charge level influences the overall mass deposits on both of the blade sides, in particular the OC allows a consistent reduction of the mass deposits. The reduction is in the range of (39–50)% depending on the environmental conditions.

These results highlight the importance of the presence of the filtration system and its efficiency:

— the filtration system with PC reduces the mass contaminant by about 78% on the PS and by about 54% on the SS with respect to the case without filtration system;
— the filtration system with OC reduces the mass contaminant by about 88% on the PS and by about 72% on the SS with respect to the case without filtration system.

Finally, it is possible to observe that the characterization of the contaminant concentration in the air is more important than the

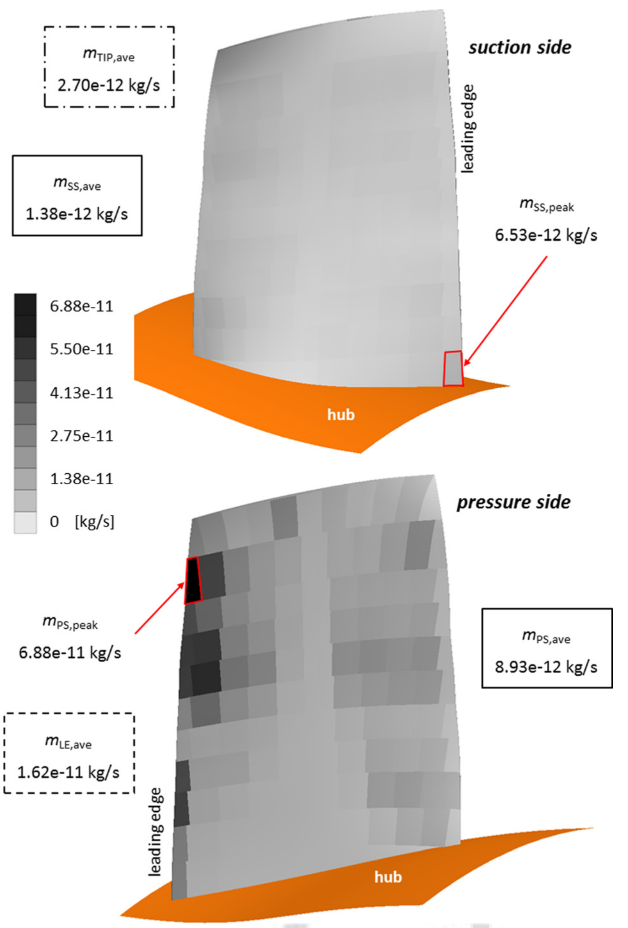

Fig. 12 Overall deposits on the blade surface without filtration system

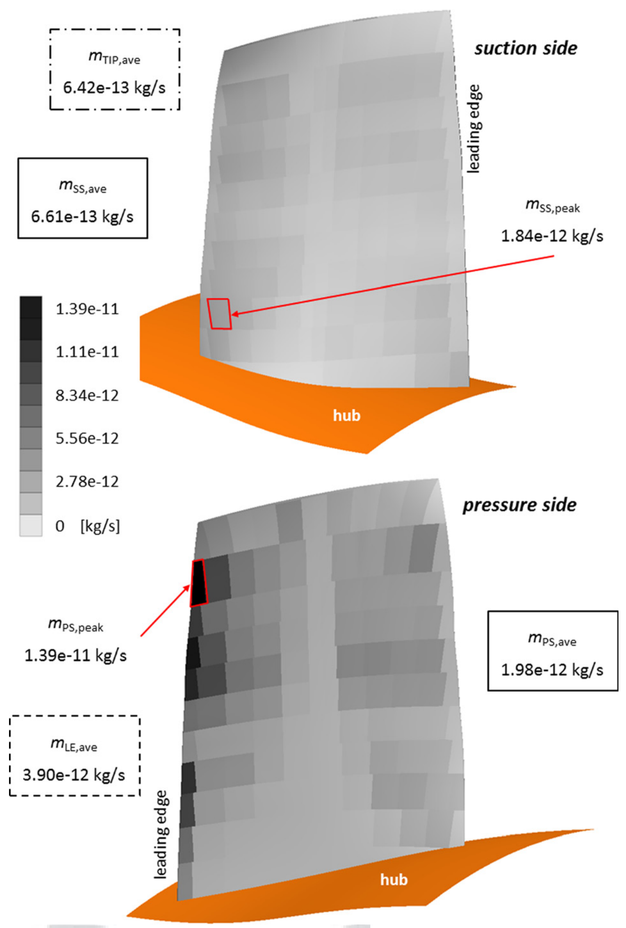

Fig. 13 Overall deposits on the blade surface: IS and PC

filter charge. In fact, IW and/or Urban conditions in the case of PC are less dangerous than the IS condition in the case of OC.

In Figs. 10 and 11, the differences in terms of particle diameter are reported for pressure suction and SS, respectively. The different charge condition determines a more flat scenario with respect to the single particle diameter. This effect is more evident in the PS than in the SS. For example, for the IS condition, in case of PC the highest contribution corresponds to $d_p = 1.00\,\mu$m, while in case of OC, the contributions of the particle with a diameter in the range (0.15–1.00) μm are quite similar. In the SS, the higher contribution is related to particles with a diameter equal to 0.15 μm and 0.25 μm during the IS condition. Regarding the SS, it is important to emphasize that the smallest particles are the most dangerous only for the IS condition while, in the IW and Urban conditions, the most dangerous particles are 0.50 μm and 0.25 μm, respectively.

Overall Deposits. In this section, the authors have reported a specific analysis related to the deposits on the blade surface. As mentioned above, the blade surface was divided into 11 strips along the spanwise direction, and into 12 slices along the chordwise direction. This very fine discretization of the blade surface allows the visualization of deposits which is quite similar to the real scenario.

For each considered case, the localization of the contaminant peak on the pressure side ($m_{PS,peak}$) and suction side ($m_{SS,peak}$) is reported. The average values of contaminant at the pressure side ($m_{PS,ave}$) suction side ($m_{SS,ave}$), leading edge ($m_{LE,ave}$), and blade tip ($m_{TIP,ave}$) are also reported. The deposits on these blade areas in fact have the greatest influence in compressor performance degradation, as reported in Refs. [19] and [20].

Without Filtration System. In a similar manner to analyses reported in the previous section, the first analysis is carried out in order to set the reference. In fact, the results reported in Fig. 12 show the blade contamination in the absence of the filtration system. Figure 12 shows that the deposits are concentrated in the first part of the airfoil chord on the PS. In particular, the peak value is in correspondence with the LE: in the PS at the tenth strip (83% of the blade span) while in the SS it is at the first strip (3% of the blade span). The deposits on the SS are more distributed with respect to those on the PS, but the average value is an order of magnitude less than the PS. At the blade tip, the average value of deposit is higher than the average values of the SS. This implies that the blade tip is more fouled with respect to the SS. AQ5

IS and PC. The second analysis refers to the most dangerous fouling operating condition: PC of the filtration system and IS as the compressor work environment. Comparing this result to the case without filtration system, it is possible to understand the importance of the filtration system even if its efficiency is not optimal. This condition is usual in the case of fully loaded power units for which the shut-off is not possible. Figure 13 shows the deposits on the blade surface. The colorbar values are different from the previous case in order to improve the contour plot readability. The colorbar values used for this analysis will be held constant for all the following analyses.

The peak value in the PS is located in the same area as the previous case with a reduction in mass contaminant of about 80%. On the SS, the deposit peak is located in the rear part of the airfoil chord at the third strip (21% of the blade span) with a reduction of about 72% with respect to the case without a filtration system. Regarding the average values of the deposits in the PS and SS, it can be noticed that the filtration system with a PC realizes a

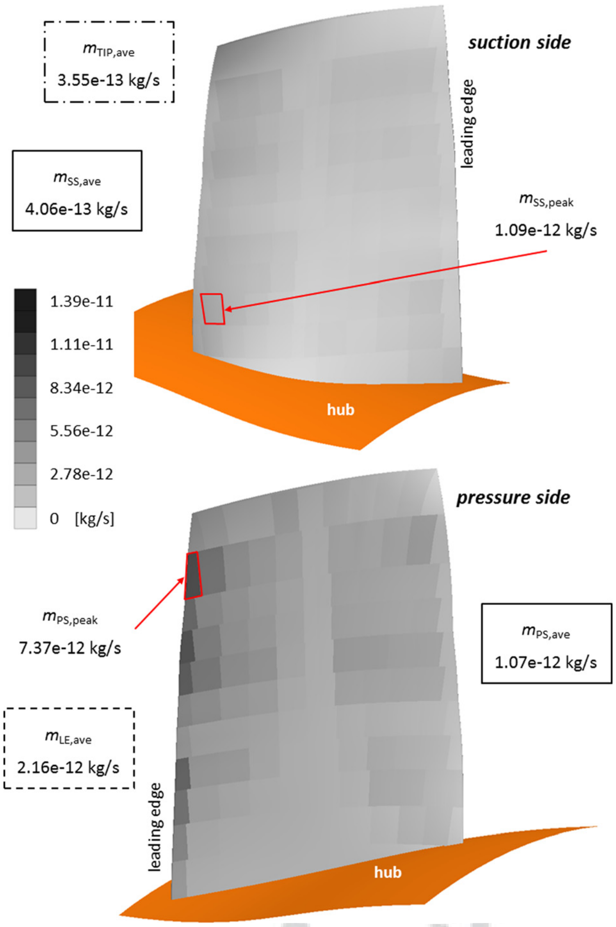

Fig. 14 Overall deposits on the blade surface: IS and OC

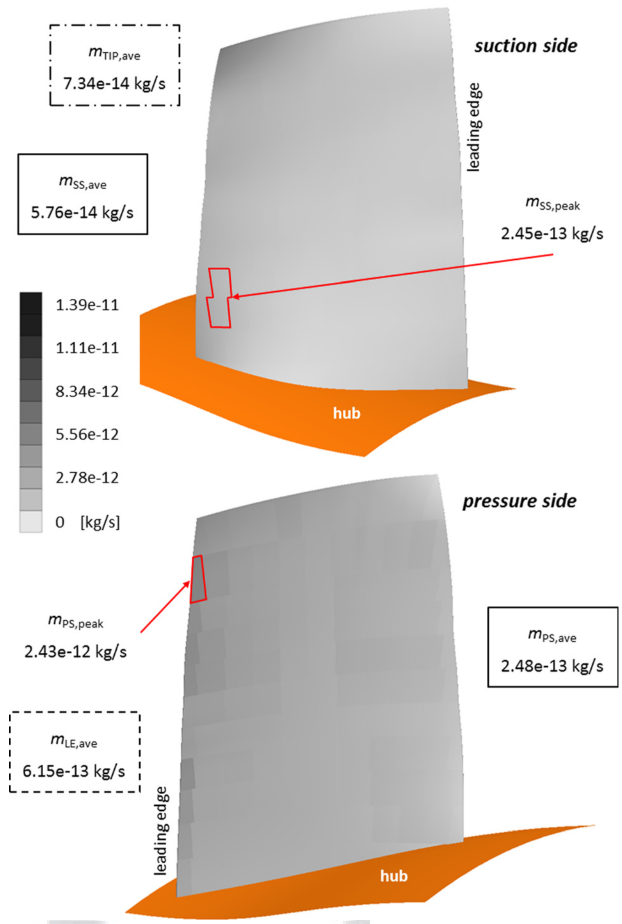

Fig. 15 Overall deposits on the blade surface IW and OC

reduction of about 78% of the mass deposits on the PS, while on the SS the reduction is only about 52%.

Finally, the filtration system seems to determine a spreading of deposits in the SS. In fact, the peak value and the average one are closer to each other and the difference is only about 64% with respect to the peak value.

IS and OC. The third analysis is conducted in order to emphasize the performance and the benefits deriving from the proper management of the filtration system. Figure 14 shows the deposits on the blade surface in the case of IS environment with OC conditions. As mentioned above, the filtration system charge reduces the amount of deposits on the blade surface. For the PS the average reduction is about 46% while for the SS the reduction is about 39% with respect to the case with the PC condition. Again, the influence of the filtration system is higher for the PS than for the SS. The peak values in the PS and SS are in the same blade areas with respect to the previous cases (without filtration system, and IS with PC). Once again, the SS appears uniformly contaminated and the spread effect due to the filtration system is present. The difference between the peak value and the average value on the SS is similar to the previous case (about 63% with respect to the peak value). On the SS, the blade area close to the blade tip (tenth strip, 83% of the blade span) is also affected by deposits in a similar way to the peak value area.

IW and OC. The last analysis refers to the least heavy operating condition: IW environment with the OC conditions. Figure 15 shows the deposits on the blade surface. As mentioned above, this condition is the least heavy of those considered. In this case, the contaminant concentration in the ingested air has a greater influence for the deposits in the SS: the reduction of the peak value is equal to 78% for the SS (with respect to the peak value resulting for the case IS with OC), while in the PS the reduction of the peak value is about 67% (with respect to the peak value resulting for the case IS with the OC). The same trend can be obtained by using the average values. For these reasons, air contamination plays a key role in the performance degradation because the deposits on the SS have a greater influence on the compressor performance drop [19]. In the light of this consideration, Fig. 16 shows that the SS areas are interested by the deposits (dark-gray colored) and the blade areas are not interested by the deposits (pale-gray colored). Figure 16(*a*) represents the first three cases: (i) IS without filtration system, (ii) IS with PC, and (iii) IS with OC, while Fig. 16(*b*) refers to IW with OC. As mentioned above air contamination has the greatest influence for the SS. In fact, as can be seen in Fig. 16, only the variation of the air contaminant concentration can influence the pattern of deposits on the SS.

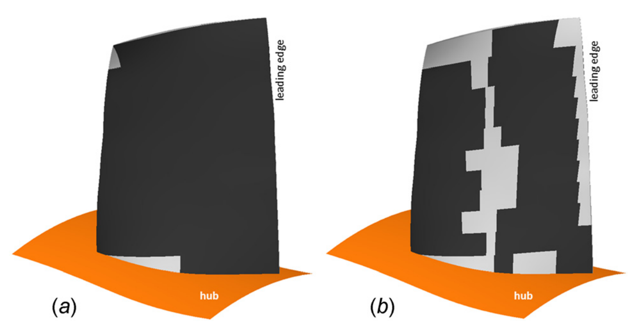

Fig. 16 Deposits pattern on the SS: (*a*) IS without filtration system, IS with PC and IS with OC and (*b*) IW with OC

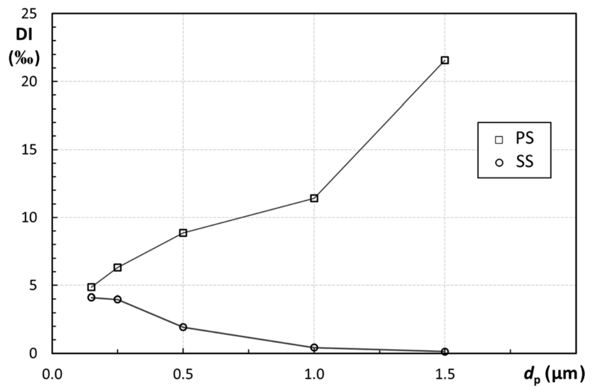

Fig. 17 DI versus particle diameter

Observations

AQ6 Mass deposits reported in previous sections pointed out that, for both rotors, PS is more contaminated by the deposits than the SS, beyond the season and the filtration efficiency. Mass deposits are influenced in greater manner by bigger particles ($d_p = 1.00\,\mu m$ and $d_p = 1.50\,\mu m$) inasmuch the mass deposits are related to (i) particle diameter, (ii) number of particle, and (iii) the average value of the SP because the particle density is kept constant.

Values of the mass deposits presented in this work are directly related to the DI. As mentioned above, this index is strongly related to the sticking coefficient reported in Ref. [18]. By using the DI, it is possible to point out some considerations about the particle adhesion on the pressure and SS for both rotors and comparing the results with the discussion reported in Ref. [18]. Even if in Ref. [18] the cascade under investigation refers to a gas turbine, some general hints could be used for explaining the results presented in this work.

Figure 17 shows the relationship between the DI and the particle diameter for the PS and SS. It is clearly visible the different effects of the flow field on the particle deposition. As reported in Ref. [18], inertial deposition takes a place on the pressure surface for diameter greater than 1 μm and, by contrast, the SS is affected by diffusion deposition provided by the diameters less than 1 μm.

In a transonic rotor, where the flow field is greatly different from the PS and SS, the DI assumes different values and, for the SS, its values are very low for bigger diameter. In the SS in fact, the separation, due to the shock wave, determines a turbulent and thicker boundary layer. This condition allows the diffusion–deposition condition and, as reported in literature, this condition influences the deposition of the smaller particles [12]. On the PS, the inertia deposition takes a place, and for this reason, the DI increases as particle diameter increases.

Since this analysis, even if (i) the particle's characteristics used in Ref. [17] are different from those involved in the fouling phenomena, (ii) the simplification adopted in this work and in Refs. [15] and [16] such as particle's density, particle's diameter, the deposition trends (Fig. 17) are in agreement with the experimental results reported in the literature [18] demonstrating that the combination of the interdisciplinary results could be an effective strategy to look over at the fouling phenomenon.

Considering all the analyses, some general rules can be drawn:

— The PS is more affected by the deposits in the first part of airfoil chord (close to the LE) at the top of the blade (about 80% of blade span). On this side, the deposits do not cover the entire surface and some blade areas remain almost completely free from deposits (especially in the midchord zone, full span).

— The SS is more affected by the deposits in the areas close to the hub for the full chord length. On this side, the deposits appear much more uniform and there is not a preferable blade area interested by the contaminant;

— The filtration system influences the deposition rate: the presence and/or the operating conditions of the filtration system determine the amount of deposit that affected each blade area. Its influence appears more relevant for the PS deposition rate.

— The work environment of the compressor determines that the blade areas are interested by the deposits. Different air contaminant concentrations lead to different fouled blade areas. Their influence appears more relevant for the SS deposition rate.

Conclusions

In this paper, an estimation of the actual deposits on the blade surface in terms of location and quantity is proposed. The deposits on the blade surface lead to actual (i) particle diameters, (ii) air contaminant concentrations, and (iii) filtration efficiency in order to perform a realistic quantitative analysis of the fouling phenomena in an axial compressor. The results show a combination of the impact/adhesion characteristics of the particles (obtained through CFD numerical simulations) and the real size distribution of the contaminants in the air.

The results show the different effects induced by the filtration system and the work environment of the compressor on the deposition rate and on the blade surface deposition pattern. In general, the PS results affected more at the top of the blade, while the deposits on the SS appear distributed more on the blade surface. The filtration efficiency induces a reduction of the deposition rate and its influence is more relevant for the PS. The work environment of the compressor strongly characterizes the deposition pattern in the SS.

Through these analyses, it is possible to determine the evolution of the fouling phenomenon by the integration of (i) CFD numerical analysis (that provides the match between the design characteristic of the machine and the fluid-dynamic phenomena) and (ii) power plant characteristics (air contaminant concentrations and the efficiency of filtration systems).

In the future, this approach could be a support in the preliminary design phase, in order to establish, a priori, the cost management due to the maintenance of filtration systems, the interval for washing operations as a function of the axial compressor and the air contaminant concentration that characterizes the power plant location.

Nomenclature

d = diameter
m = mass flow rate
n = ratio
P = number of particle

Greek Symbols

η = efficiency
χ = contaminant concentration

Subscripts and Superscripts

ave = average value
f = filtration system
max = maximum value
min = minimum value
p = particle
peak = peak value

Acronyms

CFD = computational fluid dynamics
DI = dangerous index
IS = industrial spring

IW = industrial winter
LE = leading edge
OC = optimal charge
PC = poor charge
PS = pressure side
SEM = scanning electron microscope
SP = sticking probability
SS = suction side
TE = trailing edge
U = Urban

References

[1] Kurz, R., and Brun, K., 2012, "Fouling Mechanism in Axial Compressors," ASME J. Eng. Gas Turbines Power, **134**(3), p. 032401.

[2] Suder, K. L., Chima, R. V., Strazisar, A. J., and Roberts, W. B., 1995, "The Effect of Adding Roughness and Thickness to a Transonic Axial Compressor Rotor," ASME J. Turbomach., **117**(4), pp. 491–505.

[3] Gbadebo, S. A., Hynes, T. P., and Cumpsty, N. A., 2004, "Influence of Surface Roughness on Three-Dimensional Separation in Axial Compressors," ASME J. Turbomach., **126**(4), pp. 455–463.

[4] Kurz, R., Brun, K., Meher-Homji, C., and Moore, J., 2012, "Gas Turbine Performance and Maintenance," 41st Turbomachinery Symposium, Houston, TX, Sept. 24–27, pp. ■–■. AQ7

[5] Vigueras, Z., and Marco, O., 2007, "Analysis of Gas Turbine Compressor Fouling and Washing on Line," Ph.D. thesis, Cranfield University, ■, UK. AQ8

[6] Brice, T., "Atmospheric Aerosols: Physical Properties; Chemical Composition; Health & Environmental Effects," Department of Chemistry, UCC, Ireland.

[7] Lü, S., Zhang, R., Yao, Z., Yi, F., Ren, J., Wu, M., Feng, M., and Wang, Q., 2012, "Size Distribution of Chemical Elements and Their Source Apportionment in Ambient Coarse, Fine, and Ultrafine Particles in Shanghai Urban Summer Atmosphere," J. Environ. Sci., **24**(5), pp. 882–890.

[8] Lu, S., Yi, F., Hao, X., Yu, S., Ren, J., Wu, M., Jialiang, F., Yonemochi, S., and Wang, Q., 2013, "Physicochemical Properties and Ability to Generate Free Radicals of Ambient Coarse, Fine, and Ultrafine Particles in the Atmosphere of Xuanwei, China, an Area of High Lung Cancer Incidence," Atmos. Environ., **97**(■), pp. 519–528.

[9] Wilcox, M., Baldwin, R., Garcia-Hernandez, A., and Brun, K., 2010, "Guideline for Gas Turbine Inlet Air Filtration Systems," Gas Machinery Research Council Southwest Research Institute, Release 1.0.

[10] Tarabrin, W. P., Schurovsky, V. A., Bodrov, A. I., and Stalder, J.-P., 1998, "Influence of Axial Compressor Fouling on Gas Turbine Unit Performance Based on Different Schemes and With Different Initial Parameters," ASME Paper No. 98-GT-416.

[11] Syverud, E., Brekke, O., and Bakken, L. E., 2005, "Axial Compressor Deterioration Caused by Saltwater Ingestion," ASME Paper No. GT2005-68701.

[12] Parker, G. J., and Lee, P., 1972, "Studies of the Deposition of Sub-Micron Particles on Turbine Blades," Proc. Inst. Mech. Eng., **186**(1), pp. 519–526.

[13] Elrod, C. E., and Bettner, J. L., 1983, "Experimental Verification of an Endwall Boundary Layer Prediction Method," Report No. AGRAD CP-351.

[14] Tarabrin, A. P., Schurovsky, V. A., Boldrov, A. I., and Stalder, J.-P., 1998, "An Analysis of Axial Compressor Fouling and a Blade Cleaning Method," ASME J. Turbomach., **120**(2), pp. 256–261.

[15] Suman, A., Morini, M., Kurz, R., Aldi, N., Brun, K., Pinelli, M., and Spina, P. R., 2014, "Quantitative CFD Analyses of Particle Deposition on a Transonic Axial Compressor Blade—Part II: Impact Kinematics and Particle Sticking Analysis," ASME J. Turbomach., **137**(2), p. 021009.

[16] Suman, A., Kurz, R., Aldi, N., Morini, M., Brun, K., Pinelli, M., and Spina, P. R., 2014, "Quantitative CFD Analyses of Particle Deposition on a Transonic Axial Compressor Blade—Part I: Particle Zones Impact," ASME J. Turbomach., **137**(2), p. 021010.

[17] Poppe, T., Blum, J., and Henning, T., 2000, "Analogous Experiments on the Stickiness of Micron-Sized Preplanetary Dust," Astrophys. J., **533**(1), pp. 454–471.

[18] Ahluwalia, R. K., Im, K. M., and Wenglarz, R. A., 1989, "Flyash Adhesion in Simulated Coal-Fired Gas Turbine Environment," ASME J. Eng. Gas Turbines and Power, **111**(4), pp. 672–678.

[19] Morini, M., Pinelli, M., Spina, P. R., and Venturini, M., 2011, "Numerical Analysis of the Effects of Non-Uniform Surface Roughness on Compressor Stage Performance," ASME J. Eng. Gas Turbines Power, **133**(7), p. 072402.

[20] Aldi, N., Morini, M., Pinelli, M., Spina, P. R., Suman, A., and Venturini, M., 2014, "Performance Evaluation of Non-Uniformly Fouled Axial Compressor Stages by Means of Computational Fluid Dynamics Analyses," ASME J. Turbomach., **136**(2), p. 021016. AQ9